PHYSICAL REVIEW B VOLUME 16, NUMBER 8 15 OCTOBER 1977

Theory of surface-mode phonon amplification in piezoelectric semiconductor films

Shin-ichiro Tamura and Tetsuro Sakuma
Department of Engineering Science, Hokkaido University, Sapporo 060, Japan
(Received 25 April 1977)

Amplification characteristics of surface-mode elastic waves in piezoelectric semiconductor films are investigated quantum mechanically in the microwave-frequency region, i.e., 10–100 GHz. We assume that the mediums are isotropic elastically and that a quasi-free-electron description of the conduction electrons is valid. Both the deformation-potential coupling and the piezoelectric coupling are considered to describe the electron–surface-mode-phonon interaction. Numerical examples are developed for an n-type GaAs epitaxial layer on a semi-insulating GaAs substrate at $T = 77$ K. Frequency dependence of amplifications will be discussed in comparison with those of the bulk and the surface (Rayleigh) waves.

I. INTRODUCTION

Elastic surface waves (ESW) have been the subject of considerable interest both in surface physics and microwave electronics. The ESW can be used as a probe for understanding the properties of solids near their surfaces such as surface electronic states,[1] surface irregularities,[2] and surface modes of elementary excitations.[3] In the field of microwave electronics the ESW provide possibilities for minimizing the devices several orders of magnitude compared with their electromagnetic counterparts and to develop new types of acoustic devices, i.e., surface-wave devices, which promise wider applications.[4] From the viewpoint of an application to microwave electronics, the amplification of the ESW is very important, especially in the GHz frequency region.

Recently, the present authors have investigated theoretically the amplification characteristics of Rayleigh waves in piezoelectric semiconductor films.[5] In Ref. 5 the amplification of Rayleigh waves with frequencies of 1–10 GHz has been formulated quantum mechanically. In consequence, we have found that the frequency dependences of the Rayleigh-wave amplification coefficients ($\alpha \sim \omega^{4.3}$–$\omega^{4.7}$ for $ql \simeq 1$ and $q < k_D$, where ω, q, l, and k_D are the angular frequency, the wave number, the mean free path of electrons, and the reciprocal of the Debye length, respectively) are considerably different from those of the bulk wave obtained assuming only the piezoelectric coupling ($\alpha \sim \omega^3$ for $ql > 1$, $q < k_D$ and $\alpha \sim \omega^2$ for $ql < 1$, $q < k_D$).[6]

It is well known that in an isotropic elastic medium with a stress-free plane boundary, there exist four different kinds of elastic waves other than the Rayleigh (surface) wave (R mode). They are often referred to as the P-SV (pressure wave–shear wave with vertical polarization) mode wave, the SV-P mode wave, the TR (total reflection) mode wave, and the SH (shear wave with horizontal polarization) mode wave (see Fig. 1).

We briefly account for these four mode waves, which we call surface-mode waves hereafter. If a pressure wave (P wave) propagating in a medium is incident to the stress-free boundary surface, a pressure wave and a shear wave polarized in the vertical plane (SV wave) come out as the reflected waves from the surface. We call this mode the

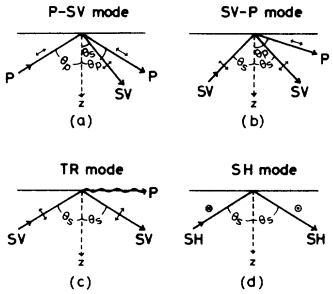

FIG. 1. Surface-mode waves other than the Rayleigh mode wave: P, pressure (longitudinal) wave; SV, shear (transverse) wave polarized in the vertical plane; SH, shear wave polarized in the horizontal plane. (a) P-SV mode consists of an incident P wave (incidence angle θ_p) and reflected P (reflection angle equal to incidence angle θ_p) and SV (reflection angle θ_s) waves. (b) SV-P mode consists of an incident SV wave and reflected SV and P waves. In this mode, a critical angle θ_c for the incident SV wave exists. The θ_c is the value of θ_s when the reflection angle θ_p of the P wave reaches $\frac{1}{2}\pi$. (c) TR (total reflection) mode may be understood as a mode which appears when the angle of incidence θ_s exceeds θ_c in the SV-P mode. The reflected P wave travels along the surface of a medium and penetrates into the medium only about a wavelength from the surface (i.e., total reflection). (d) In SH mode, both an incident and a reflected wave are SH waves with the same angle of incidence and reflection. The SH wave is polarized perpendicular to the surface of the paper.

P-SV mode. The angles of incidence and reflection of the P wave are equal to each other (θ_p), and the angle of reflection θ_s of the SV wave is smaller than θ_p because the shear wave travels more slowly than the P wave. On the other hand, if the SV wave is incident to the boundary surface with a small angle of incidence, the SV wave and the P wave appear as the reflected waves from the surface. This is referred to as the SV-P mode. Also in this mode, both the angles of incidence and reflection of the SV waves have the same value θ_s. It should be noted that in this mode there exists the critical angle θ_c. θ_c is the angle of incidence of the SV wave for which the angle of reflection of the P wave becomes just 90°. For the angle θ_s of the SV waves larger than θ_c the SV-P mode reduces to the TR mode. Therefore the TR mode can be understood as the special case of the SV-P mode in which the SV wave is incident to the surface with the angle of incidence θ_s larger than θ_c and the P wave is totally reflected by the surface. In this mode the amplitude of the P wave decays exponentially away from the surface. Finally, if we project the shear wave polarized in the horizontal plane (SH wave) to the plane boundary surface, the SH wave is reflected from it with the same angle of reflection as that of incidence. No other wave than the SH wave appears as the reflected waves, because the particle displacements of the SH wave are parallel to the surface.

The purpose of the present paper is to investigate the amplification of these surface-mode waves by the electrons confined in a semiconductor film. We are interested in the microwave frequency region, and here we consider the waves of frequencies from 10 to 100 GHz. At such high frequencies, the pressure-wave component of the TR mode wave which travels along the surface is localized within 1000 Å or less from the surface. Since the electronic states of a semiconductor in this vicinity of its surface are not so simple and their detailed structures are very important for specifying the interaction of the TR mode wave with electrons, the TR mode wave will not be discussed simultaneously with three other mode waves. Therefore, in this paper we shall restrict our discussion to the amplifications of three surface-mode waves other than the TR mode waves, that is, the P-SV, SV-P, and SH mode waves.

As in our previous papers,[5] a surface-mode-wave amplifier is assumed to have a layered structure consisting of an epitaxial film of a piezoelectric semiconductor and an insulating substrate. Since the surface-mode waves defined in this paper cannot exist as eigenmodes of the elastic waves in the medium where the film and the substrate have different elastic properties, we choose the substrate as the same kind of semiconductor in its elastic property as the film but of an insulating nature. A typical example with such a layered structure is a system of an n-type GaAs film epitaxially grown on a semi-insulating GaAs substrate. From now on, we consider the system of the above-mentioned structure and assume the thickness of the film to be 10 μm. It is also assumed that the materials are isotropic in their elastic properties. Of course, the real medium (e.g., GaAs) has an elastic anisotropy; so the isotropic approximation will be used in the numerical calculations.

As we shall see later, the product ql takes a value much larger than unity in the frequency region considered here; therefore we should employ quantum mechanics to formulate the whole problem. On the other hand, $\omega\tau$ (τ is the relaxation time of electrons) is about unity or less than unity. Therefore, in a calculation of the amplification rate, the effect of the finite relaxation time of electrons might be important. In the second paper of Ref. 5, however, it has been shown that the effect is indeed crucial both for the magnitudes and the frequency dependences of the amplification coefficients at frequencies near 1 GHz, but, at least insofar as the qualitative characteristics of the amplification are concerned, we may neglect it at frequencies above 10 GHz. We can therefore use the Born approximation of perturbation theory in the calculation of the amplification rate.

In the next section, we describe the configuration of the amplifier and specify the wave function of the electrons. In Sec. III, a brief report on a quantum version of the surface-mode waves (surface-mode phonons) is presented. In Sec. IV, we write the electron–surface-mode-phonon interaction. Section V is devoted to the derivation of the amplification rate. In Sec. VI, the numerical analyses are developed for the epitaxial layer of an n-type GaAs on a semi-insulating GaAs substrate. A summary and a discussion will be given in the last section. In the Appendix we present the derivation of the potentials induced piezoelectrically by the surface-mode waves.

II. ELECTRONIC STATES IN A SEMICONDUCTOR LAYER

The configuration of the amplifier that we consider for amplification of the surface-mode waves is depicted in Fig. 2. A thin layer (thickness a) of a piezoelectric semiconductor is grown epitaxially on an insulating substrate with the same elastic properties as the semiconductor layer. The Cartesian coordinates are fixed so that the material occupies the half-space $z \geq 0$ and has the stress-

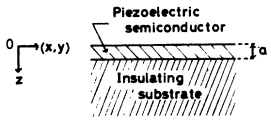

FIG. 2. Schematic drawing of the amplifier consisting of a layered structure of a piezoelectric semiconductor and an insulating material.

free surface parallel to the x-y plane.

We assume that a quasi-free-electron description of the conduction electrons is valid, so that in this configuration we might approximate the motions of electrons parallel to the surface by plane waves. On the other hand, the motions perpendicular to the surface may not be described simply by the plane waves, but will rather be described by some kind of standing waves which are determined depending on the structure of the potential-confining electrons within the semiconductor film. It is known that there exist depletion layers on both sides of the semiconductor film near its surface and the substrate. A typical thickness of these layers is about 0.3 μm for the mean electron concentration of $10^{16}/\mathrm{cm}^3$; it can be neglected in comparison with the 10-μm thickness of an epitaxial semiconductor film, which we shall take as a typical one. Here, we also note that the energy gaps of semi-insulating or intrinsic semiconductors are of order 1 eV, which is large compared with the thermal energies of the conduction electrons at $T = 77$ K.[7] Taking these facts into account, we assume in the first approximation that the carrier electrons are bounded in the film by a square-well potential with infinite barriers at $z = 0$ and $z = a$. Under this approximation, we obtain the wave function $\Psi(\vec{r})$ of the conduction electrons as

$$\Psi(\vec{r}) = \frac{1}{\sqrt{S}} \sum_{n=1}^{\infty} \sum_{\vec{p}} \phi_n(z) e^{i\vec{p}\cdot\vec{x}}, \tag{1}$$

with

$$\phi_n(z) = (2/a)^{1/2} \sin(n\pi z/a), \quad n = 1, 2, \ldots \tag{2}$$

where $\vec{r} = (\vec{x}, z) = (x, y, z)$, $\vec{p} = (p_x, p_y)$, and S is a surface area. The energies of the electronic states specified by $\vec{p}$ and n are given by

$$E_n(\vec{p}) = \hbar^2 \vec{p}^2/2m + \epsilon_n, \tag{3}$$

with

$$\epsilon_n = (\pi\hbar n)^2/2ma^2, \tag{4}$$

where m is the effective mass of the conduction electrons (assuming a spherical constant energy surface). For $a = 10$ μm, the thickness of an expitaxial film, and $m = 0.07m_0$ (m_0 being the mass of the free electron and $0.07m_0$ the effective mass of the electron of GaAs), we have $\epsilon_n = 5.38 \times 10^{-8} n^2$ eV. On the other hand, the phonon energy at frequency 10 GHz is 4.14×10^{-5} eV. Since $\epsilon_n - \epsilon_{n-1} = 1.08 \times 10^{-7}(n - \frac{1}{2})$ eV, the discreteness of the quantized electronic energy levels becomes relevant only for the electronic states with $n \gtrsim 400$ for the phonon of 10 GHz frequency. In the numerical examples of Sec. VI, we shall see that electronic states up to $n \simeq 800$ contribute to the amplifications of the surface-mode waves, so that we do not replace the discrete sum over n by an integral over a continuous variable.

Now, the field operator $\psi(\vec{r})$ of electrons is written, in the second-quantized form, as

$$\psi(\vec{r}) = \frac{1}{\sqrt{S}} \sum_{n=1}^{\infty} \sum_{\vec{p}} b_{\vec{p},n} \phi_n(z) e^{i\vec{p}\cdot\vec{x}}, \tag{5}$$

where $b_{\vec{p},n}$ and its Hermitian conjugate $b^{\dagger}_{\vec{p},n}$ are annihilation and creation operators of the electrons which satisfy commutation relations of the Fermi type.

III. SURFACE-MODE PHONONS

As was mentioned in the Introduction, there exist five eigenmodes of elastic waves in an isotropic elastic medium occupying a half-space with a stress-free plane boundary. In the quantization of such surface and the surface-mode waves, we must find a complete orthonormal set of eigenwaves. The P-SV and SV-P modes are degenerate with respect to wave velocities, and their wave functions are not orthogonal to each other (they are, of course, orthogonal to the other three modes.) The two of the members which constitute the complete set are not the P-SV and SV-P modes, but rather the so-called plus (+) and minus (−) modes which are appropriate combinations of those two modes and are orthogonal to each other.[8]

Using a complete set constructed in such a manner, we can expand the displacement vector $\vec{u}(\vec{r}, t)$ of the medium in the configuration shown in Fig. 2 as

$$\vec{u}(\vec{r}, t) = \sum_{J} \left(\frac{\hbar}{2\rho\omega_J S}\right)^{1/2} [a_J \vec{u}_J(\vec{r}) e^{-i\omega_J t} + \text{H.c.}], \tag{6}$$

where ρ is the mass density of medium and $J = (\vec{k}, \mu, c)$ is a suitable set of quantum numbers, $\vec{k} = (k_x, k_y)$ is a wave vector parallel to the surface ($x - y$ plane), μ specifies five propagation modes (R, +, −, TR, and SH), and c is a phase velocity defined by $\omega_J = c|\vec{k}| = ck$. The sum over J is to be understood to be[9]

$$\sum_{J} f(J) = \sum_{\vec{k}} \left(\sum_{\mu \neq R} \int_{D_\mu} \frac{dc}{c} f(\vec{k}, \mu, c) + f(\vec{k}, R, c_R) \right). \tag{7}$$

D_μ denotes the range of the velocities c for the mode μ. a_J and its Hermitian conjugate $a_J^\dagger$ are the annihilation and creation operators of the surface and the surface-mode phonons (quanta of the surface and the surface-mode waves), which commute with each other except for the case

$$[a_J, a_{J'}^\dagger] = \delta_{JJ'}, \quad \delta_{JJ'} = \delta_{\vec{k}\vec{k}'}\delta_{\mu\mu'}\delta_{cc'}. \tag{8}$$

If c and c' belong to the continuous spectrum, we understand $\delta_{cc'}$ as $\delta_{cc'} = c\delta(c-c')$. For explicit expressions of the wave functions $\vec{u}_J(\vec{r})$, we refer to the paper of Ezawa,[8] but for our purpose we write down three of them for the propagation modes P-SV, SV-P, and SH.[10] For the P-SV mode

$$\begin{aligned} u_J^j(\vec{r}) &= -k_j(1/2\pi k)^{1/2}[\delta^{-1/2}(e^{-i\delta kz} - De^{i\delta kz}) \\ &\quad + \sigma^{1/2}Be^{i\sigma kz}]e^{i\vec{k}\cdot\vec{x}}, \\ u_J^z(\vec{r}) &= (k/2\pi)^{1/2}[\delta^{1/2}(e^{-i\delta kz} + De^{i\delta kz}) \\ &\quad + \sigma^{-1/2}Be^{i\sigma kz}]e^{i\vec{k}\cdot\vec{x}}, \end{aligned} \tag{9}$$

for the SV-P mode

$$\begin{aligned} u_J^j(\vec{r}) &= ik_j(1/2\pi k)^{1/2}[\delta^{-1/2}Be^{i\delta kz} \\ &\quad + \sigma^{1/2}(e^{-i\sigma kz} + De^{i\sigma kz})]e^{i\vec{k}\cdot\vec{x}}, \\ u_J^z(\vec{r}) &= i(k/2\pi)^{1/2}[\delta^{1/2}Be^{i\delta kz} \\ &\quad + \sigma^{-1/2}(e^{-i\sigma kz} - De^{i\sigma kz})]e^{i\vec{k}\cdot\vec{x}}, \end{aligned} \tag{10}$$

and for the SH mode

$$\begin{aligned} u_J^x(\vec{r}) &= -k_y(2c^2/\pi c_t^2\sigma k)^{1/2}\cos\sigma kz\, e^{i\vec{k}\cdot\vec{x}}, \\ u_J^y(\vec{r}) &= k_x(2c^2/\pi c_t^2\sigma k)^{1/2}\cos\sigma kz\, e^{i\vec{k}\cdot\vec{x}}, \\ u_J^z(\vec{r}) &= 0, \end{aligned} \tag{11}$$

where $j = x, y$, and δ, σ, B, and D are constants defined by the velocities of the longitudinal wave c_l and the transverse wave c_t as well as the phase velocity c:

$$\delta^2 = (c/c_l)^2 - 1, \quad \sigma^2 = (c/c_t)^2 - 1, \tag{12}$$

$$B = \frac{4\sqrt{\sigma\delta}(\sigma^2-1)}{(\sigma^2-1)^2+4\sigma\delta}, \quad \text{and} \quad D = \frac{(\sigma^2-1)^2-4\sigma\delta}{(\sigma^2-1)^2+4\sigma\delta}.$$

IV. ELECTRON-SURFACE-MODE-PHONON INTERACTION

We must consider two kinds of electron-phonon interactions in piezoelectric semiconductors, that is, the deformation-potential coupling and the piezoelectric coupling. In the deformation-potential theory, the lattice distortion causes a change in the potential energy of a conduction electron which is proportional to the strain. In a piezoelectric material the lattice distortion also produces the electric field which is proportional to the strain. The deformation-potential coupling is known to be weaker than the piezoelectric coupling for phonons of low frequencies. However, they become of comparable strength for phonons with frequencies of about 100 GHz, so that for our purpose we must take these two interaction mechanisms into account simultaneously.

Here, we assume that the interaction Hamiltonian of the electron–surface-mode-phonon system is the same as that of the bulk-phonon case, and write it in the second-quantization representation as

$$H_I = H_D + H_P, \tag{13}$$

$$\begin{aligned} H_D &= C\int \psi^\dagger(\vec{r})\vec{\nabla}\cdot\vec{u}(\vec{r})\psi(\vec{r})d\vec{r} \\ &= \frac{C}{\sqrt{S}}\sum_J\sum_{\vec{p}}\sum_{ij} b_{\vec{k}+\vec{p},i}^\dagger b_{\vec{p},j}a_J\Delta_{ij}^J + \text{H.c.}, \end{aligned} \tag{14}$$

$$\begin{aligned} H_P &= -e\int \psi^\dagger(\vec{r})\tilde{\varphi}(\vec{r})\psi(\vec{r})d\vec{r} \\ &= \frac{4\pi e_P e}{\epsilon_0\sqrt{S}}\sum_J\sum_{\vec{p}}\sum_{ij} b_{\vec{p}+\vec{k},i}^\dagger b_{\vec{p},j}a_J\Phi_{ij}^J + \text{H.c.}, \end{aligned} \tag{15}$$

with $J = (\vec{k}, \mu, c)$, and where C, ϵ_0, and e_P are the material's deformation-potential coupling, static dielectric, and piezoelectric coupling constants. The summation over J is to be understood as in Eq. (7). An explicit expression of the electric potential $\tilde{\varphi}(\vec{r})$ in the piezoelectric interaction H_P is given in the Appendix. Also in the piezoelectric coupling we have considered the semiconductors with zinc-blende crystal structure which have only three nonvanishing components of the piezoelectric tensor e_{ijk}, i.e., $e_{14} = e_{25} = e_{36} = e_P$. Δ_{ij}^J and Φ_{ij}^J are given by

$$\begin{aligned} \Delta_{ij}^J &= -i\left(\frac{\hbar}{4\rho\delta c}\right)^{1/2}\left(\frac{c}{c_l}\right)^2 k \\ &\quad \times\int_0^a \phi_i(z)(e^{-i\delta kz} - De^{i\delta kz})\phi_j(z)dz, \\ \Phi_{ij}^J &= -\left(\frac{\hbar}{4\pi\rho c}\right)^{1/2} \\ &\quad \times\int_0^a \phi_i(z)\left[3\delta^{1/2}\left(\frac{c_l}{c}\right)^2(e^{-i\delta kz} + De^{i\delta kz}) \right. \\ &\quad \left. -B(2\sigma^{3/2} - \sigma^{-1/2})\left(\frac{c_t}{c}\right)^2 e^{i\sigma kz}\right]\phi_j(z)dz \end{aligned} \tag{16}$$

for the P-SV mode,

$$\begin{aligned} \Delta_{ij}^J &= -\left(\frac{\hbar}{4\pi\rho\delta c}\right)^{1/2}\left(\frac{c}{c_l}\right)^2 Bk\int_0^a \phi_i(z)e^{i\delta kz}\phi_j(z)dz, \\ \Phi_{ij}^J &= -i\left(\frac{\hbar}{4\pi\rho c}\right)^{1/2} \\ &\quad \times\int_0^a \phi_i(z)\left[3\delta^{1/2}B\left(\frac{c_l}{c}\right)^2 e^{i\delta kz} - (2\sigma^{3/2} - \sigma^{-1/2})\right. \\ &\quad \left. \times\left(\frac{c_t}{c}\right)^2(e^{-i\sigma kz} - De^{i\sigma kz})\right]\phi_j(z)dz \end{aligned} \tag{17}$$

for the SV-P mode, and

$$\Delta_{ij}^{J}=0\,. \tag{18}$$

$$\Phi_{ij}^{J}=-2i\left(\frac{\hbar\sigma}{\pi\rho c}\right)^{1/2}\frac{c_t}{c}\int_0^a \phi_i(z)\sin\sigma kz\;\phi_j(z)dz$$

for the SH mode. We have taken the directions of the wave vector $\vec{k}$ in the [110] direction for μ specifying P-SV and SV-P, and in the [010] direction for μ specifying SH. Since the conduction band of the unstrained semiconductor has been assumed to be spherically symmetric (as is the case of GaAs), only dilatation components of the strain contribute in the deformation-potential coupling H_D, and shear waves do not interact with electrons through the deformation potential. It should be noted that in a cubic crystal the shear waves traveling in the [111] direction [e.g., $\sigma=1/\sqrt{2}$ in Eqs. (16) and (17)] also decouple from the electrons piezoelectrically. An important result we can observe from Eqs. (16) and (17) is that there exist phase differences of $\frac{1}{2}\pi$ between the matrix elements for the scatterings by those two mechanisms of the electron–surface-mode-phonon interaction, i.e., H_D and H_P. This is the same result as in electron–bulk-phonon interaction, and consequently the two can be treated independently.

V. AMPLIFICATION RATE

We wish to discuss amplifications of the surface-mode phonons due to emissions and absorptions of them by electrons through the couplings H_D and H_P. It is known that the conduction electrons never travel freely in a semiconductor but are scattered by a variety of sources[11] before and after they emit or absorb the phonons we should observe. Accordingly, detailed calculations of the amplification rates of the surface-mode phonons require that we solve the complicated integral equations. However, in a calculation of the amplification coefficient of the Rayleigh wave, we have shown[5] that the effect of the finite relaxation time of the electrons resulting from the scatterings stated above is not so important for the surface phonons of frequencies over 10 GHz. Therefore, insofar as the qualitative features of the amplifications are concerned, it may be expected that for surface-mode phonons of frequencies above 10 GHz reliable results will also be obtained without reference to the finite relaxation time of the electrons. This means that we may employ the Born approximation of perturbation theory.

Now, to calculate the amplification rate $\tilde{\alpha}$ per unit time, we follow the method given in Ref. 5. Here, briefly recapitulate the derivation of $\tilde{\alpha}$. $\tilde{\alpha}$ is related to the width of a phonon or the spectral function of the one-particle phonon self-energy function Γ as $\Gamma_J=-\hbar\tilde{\alpha}_J$, where J denotes a set of quantum numbers defined above. Using Hamiltonians (13)–(15), and neglecting vertex corrections other than the screening effect of the electrons, we get the self-energy function Π of the surface-mode phonons as follows:

$$\Pi_J(\xi_\nu)=2\sum_{ij}\{[C(k)]^2|\Delta_{ij}^{J}|^2+g(k)^2|\Phi_{ij}^{J}|^2\}\times\int\frac{d\vec{p}}{(2\pi)^2}\int\int\frac{d\omega'd\omega''}{(2\pi)^2}\frac{f(\omega'')-f(\omega')}{\xi_\nu+\omega''-\omega'}\times A_i(\vec{p},\omega')A_j(\vec{p}-\vec{k},\omega''), \tag{19}$$

with

$$\xi_\nu=-2\nu\pi/i\beta\quad(\nu\text{ integer}),$$

and where $f(\omega)=(e^{\beta(\omega-\zeta)}+1)^{-1}$, $\beta=(k_BT)^{-1}$, $C(k)=C/\epsilon_l(k)$, and $g(k)=4\pi ee_P/\epsilon_0\epsilon_t$. $\epsilon_i(k)=1+4\pi Ne^2\beta c_i^2/\epsilon_0c^2k^2$ for $i=l$ and t, the electronic screening factors for the potentials induced by the acoustic vibrations of the longitudinal and the transverse waves, respectively. N is the electron concentration and ζ the chemical potential. In the piezoelectric coupling, ϵ_i must be taken as ϵ_l or ϵ_t depending on the coupling to the longitudinal or the transverse waves.

The spectral function $A_j(\vec{p},\omega)$ of the one-electron Green's function (j denotes the quantized levels of the electrons) will be replaced by the δ function in the Born approximation,

$$A_j(\vec{p},\omega)=2\pi\delta(\omega-\hbar^2\vec{p}^2/2m-\epsilon_j)\,.$$

The width Γ_J of the surface-mode phonons is obtained by taking the discontinuity of the self-energy function Π across the real axis of the complex ξ-plane:

$$\Gamma_J(\hbar\omega)=\frac{1}{\pi}\sum_{ij}\{[C(k)]^2|\Delta_{ij}^{J}|^2+g(k)^2|\Phi_{ij}^{J}|^2\}\times\int d\vec{p}\int d\omega'[f(\omega'-\hbar\omega)-f(\omega')]\,\delta\left(\omega'-\frac{\hbar^2\vec{p}^2}{2m}-\epsilon_i\right)\delta\left(\omega'-\hbar\omega-\frac{\hbar^2}{2m}(\vec{p}-\vec{k})^2-\epsilon_j\right). \tag{20}$$

In a situation where the electrons have a drift velocity v in the direction of the phonon wave vector $\vec{k}$ parallel to the surface, we must replace $\hbar\omega$ by $-\hbar\omega x$, with $x=v/c-1$, the drift parameter. Thus, finally we have the amplification rate $\tilde{\alpha}_J$ of surface-mode phonons per unit time as

$$\tilde{\alpha}_J = -\Gamma_J(-\hbar\omega x)/\hbar$$
$$= \frac{xc}{\pi\hbar^3}(\beta n^3)^{1/2}\sum_{ij}\{[C(k)]^2|\Delta_{ij}^J|^2 + g(k)^2|\Phi_{ij}^J|^2\}$$
$$\times\int_0^\infty dy\ \mathrm{sech}^2\left\{y^2 + \frac{\beta}{2}\left[\epsilon_i - \zeta + \frac{m}{2\hbar^2k^2}\left(\hbar\omega x - \frac{\hbar^2k^2}{2m} + \epsilon_i - \epsilon_j\right)^2\right]\right\}. \quad (21)$$

Equation (21) is valid for $\beta\hbar\omega x \ll 1$. It should be noted that the integral in Eq. (21) cannot be carried out analytically, and, furthermore, there exist double summations with respect to the level indices i and j specifying the electronic energies, so that we unfortunately cannot obtain the explicit frequency dependences of the amplification rate without performing numerical calculations.

The total amplification α_J produced by the electron–surface-mode-phonon interaction in a semiconductor film is obtained from $\tilde{\alpha}_J$ by multiplying it by the time T_μ needed for a surface-mode wave to transit the film, i.e.,

$$T_\mu = ac/\delta c_t^2 \text{ for the P-SV mode}$$
$$= ac/\sigma c_t^2 \text{ for the SV-P and SH modes.} \quad (23)$$

VI. NUMERICAL EXAMPLES

In this section, we develop numerical examples of the surface-mode-phonon amplifications for an n-type GaAs film grown epitaxially on a semi-insulating GaAs substrate at $T = 77$ K. The following set of parameters are taken: $e_P = 4.71\times10^4$ esu/cm^2, $C = 7$ eV, $m = 0.07m_0$ (m_0 being the mass of the free electron), $\rho = 5.32$ g/cm^3, $\epsilon_0 = 12.9$, $x = 1$, and $a = 10$ μm. In our formulation, we have assumed that the layered medium is isotropic elastically. However, the crystal GaAs is not isotropic, against our assumption.[12] So we approximate the isotropic stiffness constants from the anisotropic ones of GaAs by employing an isotropic approximation.[13]

Using those values of the approximated elastic stiffness constants, we find $c_l = 5.17\times10^5$ cm/sec and $c_t = 3.04\times10^5$ cm/sec. As for the electron concentrations, we take two typical values, $N = 1.73\times10^{15}$/cm^3 (case I) and $N = 1.07\times10^{16}$/cm^3 (case II). Corresponding values of the electron mobility are 4.99×10^4 cm^2/V sec (case I) and 1.71×10^4 cm^2/V sec (case II). We note that at 10 GHz frequency the values of the product ql are estimated to be 8.4 and 2.9 for cases I and II, respectively.

A. P-SV mode wave

GaAs has the (111) and the (001) crystal planes as its cleavages.[14] So we consider a situation which may be experimentally feasible for the P-SV mode; that is, we produce a longitudinal strain normal to the (111) plane which results in a longitudinal (or a pressure) wave propagating in the [111] direction and is incident to the surface [(001) plane]. In this configuration, the piezoelectric coupling of phonons with electrons is described just by the Hamiltonians (15) and (16), with $\tan\theta_p = \delta^{-1} = \sqrt{2}$.

The acoustic gains, or the amplifications α of the P-SV mode waves versus their frequencies, are shown in Fig. 3(a) for both electron concentrations. For case I the effect of the electronic screening is incomplete at the frequencies around 10 GHz and the frequency dependence of α is somewhat modest. On the other hand, for case II, the electronic screening is quite effective ($q \ll k_D$) in the frequency region near 10 GHz. In this region, the dependence of α on the frequency is given by $\alpha \sim \omega^{3.4}$, which should be compared with those of the bulk wave (BW), $\alpha \sim \omega^3$,[6] and the Rayleigh wave, $\alpha \sim \omega^{3.8}$,[5] obtained in the Born approximation assuming $ql > 1$ and $q < k_D$. Here, for the BW we have quoted the amplification rate derived from the piezoelectric coupling alone. For the reason stated in Sec. IV, the amplification rate due to the deformation potential is ω^2 times that obtained by the piezoelectric coupling, and for the BW the contribution of the former is proportional to ω^5.[6] Therefore, if the contribution of the deformation potential becomes effective in the frequency region where the relations $ql > 1$ and $q < k_D$ are valid, the amplification rate of the BW varies from ω^3 to ω^5. However, this is not the case, since for the values of the coupling constants given at the beginning of this section for GaAs, the deformation-potential coupling is very weak, and at frequencies near 10 GHz the amplification of the BW is determined only by the piezoelectric coupling. As we can see from Fig. 3(a), the contributions of the deformation-potential coupling to the amplifications become important in the frequency region above 30 GHz.

For case II, we see that α continues to increase up to 100 GHz. For case I, however, α has its local maximum (~16 dB) at a frequency of about 80 GHz, while at much higher frequencies the contribution of the deformation-potential coupling to α grows dominant and its frequency dependence is expected to be a positive power of ω ($\alpha \sim \omega$ for

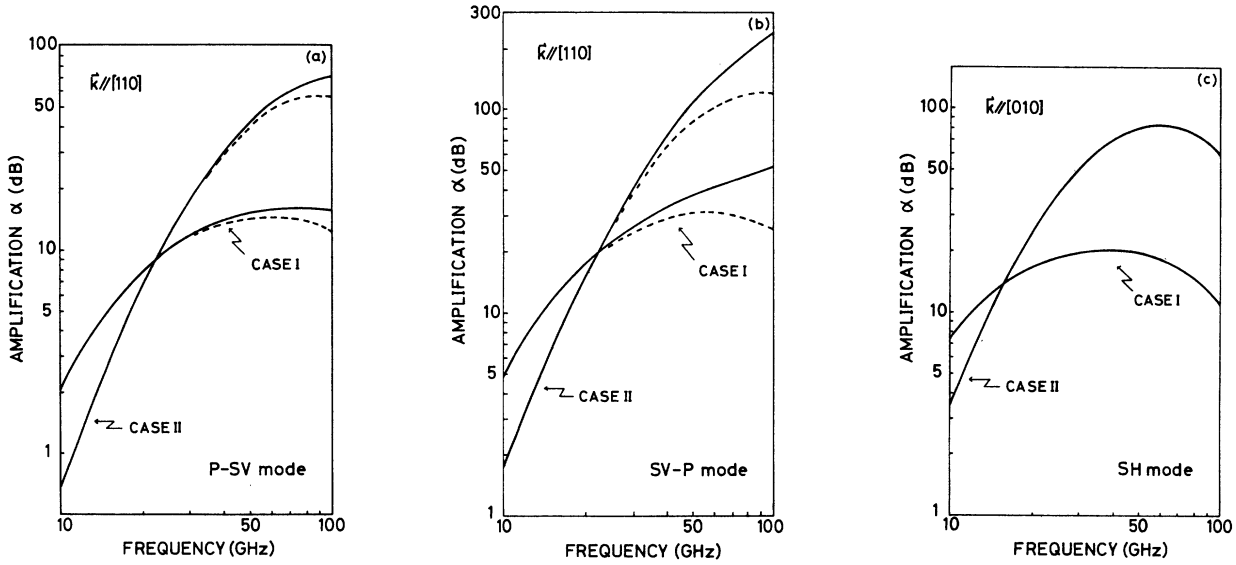

FIG. 3. Calculated curves for amplifications α of surface-mode waves at $T=77$ K and $x=v/c-1=1$. Electron concentrations are $N=1.73\times10^{15}$ cm^{-3} for case I and $N=1.07\times10^{16}$ cm^{-3} for case II. The thickness of the semiconductor film is 10 μm. Dashed curves represent contributions from the piezoelectric coupling. (a) P-SV mode wave. $\theta_p=54.74°$ ($\tan\theta_p=\sqrt{2}$). The applied electric field $E_{x=1}$ corresponding to a value of drift parameter $x=1$ is 25.4 and 74.0 V/cm for cases I and II, respectively. (b) SV-P mode wave. $\theta_s=35°$. $E_{x=1}=21.2$ V/cm for case I and 62.0 V/cm for case II. (c) SH mode wave. $\theta_s=45°$. $E_{x=1}=17.2$ V/cm for case I and 50.3 V/cm for case II.

the BW[6]), so that α will begin to rise again with frequency.

B. SV-P mode wave

The SV-P mode wave consists of an incident shear wave and reflected pressure and shear waves [see Fig. 1(b)]. Since the pressure wave propagates faster than the shear wave, there exists in this mode a critical incident angle θ_c defined by $\tan\theta_c=[(c_l/c_t)^2-1]^{-1/2}$. For $\theta_s>\theta_c$ this mode reduces to the TR mode. Using the values of c_l and c_t given above, we find $\theta_c=36.1°$. Accordingly, the amplification of the SV-P mode wave cannot be discussed in the same configuration as the P-SV mode wave (in which $\theta_s=54.7°>\theta_c$).

Unfortunately, we find no suitable configuration relying on simple crystallographic planes or axes of a cubic crystal, in which this mode wave may be efficiently amplified. Therefore, we consider here a more general situation in which we generate an SV wave with an incident angle of 35° ($<\theta_c$) and with the two-dimensional wave vector $\vec{k}$ parallel to the [110] axis. In this configuration the contribution of the deformation potential is large in comparison with that in the preceding P-SV mode wave, so that even in a rather low frequency region one might obtain information about the strength of the deformation-potential coupling from the result of the amplifications of this mode wave.

It can be found from Fig. 3(b) that for case II the frequency dependence of α is expressed as $\alpha\sim\omega^{3.3}$ at the frequencies near 10 GHz, which is very similar to the result of the P-SV mode wave. On the other hand, the frequency dependences of α near 100 GHz are approximated as $\omega^{0.5}$ and $\omega^{1.0}$ for cases I and II, respectively. We observe that at 100 GHz the curve is concave for the former and will grow steeper at higher frequencies. Therefore, it is interesting to compare these results with the amplification rate $\alpha\sim\omega$ obtained in the high-frequency limit[6] ($q\gg k_D$) for the BW assuming only the deformation-potential coupling.

C. SH mode wave

In the configurations considered for the P-SV and SV-P mode waves (i.e., $\vec{k}\parallel[110]$), the SH mode wave is not amplified (see the Appendix). Thus we must also take a configuration different from those for the previous two modes in order to see the amplification characteristics of this mode wave. For the SH mode wave with two-dimensional wave vector $\vec{k}$ pointing to the [100] and its equivalent directions, the piezoelectric coupling is simple and described by Eqs. (15) and (18), so that we consider a situation in which an SH wave with particle displacement along the [100] direction propagates in the [011] direction and is incident to the surface [(001) plane] at angle $\theta_s=45°$.

Calculated gains in this configuration are shown in Fig. 3(c). Maximum amplifications are obtained at frequencies around 40 and 60 GHz for cases I and II, respectively. For the latter, the frequency dependence of α at frequencies near 10 GHz is approximately expressed as $\omega^{3.1}$. However, we may not compare this frequency dependence with $\alpha \sim \omega^3$ of the BW, because the effect of electronic screening is thought to be incomplete for phonon frequencies of about 10 GHz. At frequencies near 100 GHz the amplifications depend on ω approximately as $\alpha \sim \omega^{-1.5}$ and $\omega^{-1.2}$ for cases I and II, respectively. These frequency dependences of α are more rapid than the amplification rate $\alpha \sim \omega^{-1}$ of the bulk shear wave[6] (which interacts with the electrons only through piezoelectric coupling) in the same frequency region where the screening effect of the electrons can be neglected.

We notice that the maximum gains of the SH mode waves are reached at frequencies lower than those at which maximum values of the dashed curves occur for the P-SV and SV-P mode waves. Here, the dashed curves represent amplifications obtained only by piezoelectric coupling. This may be accounted for by the fact that the effect of electronic screening breaks at much lower phonon frequencies for the SH mode than those of the P-SV and SV-P modes, because the shear (transverse) waves have large wave numbers in comparison with the pressure (longitudinal) waves of the same frequencies.

VII. SUMMARY AND DISCUSSION

In this paper we have studied the amplification characteristics of the microwave surface-mode (P-SV, SV-P, and SH) waves in a piezoelectric semiconductor film. It has been found in numerical examples that, for case II of the P-SV and SV-P mode waves, the frequency dependences of the amplifications at frequencies near 10 GHz are $\alpha \sim \omega^{3.3}-\omega^{3.4}$, which should be compared with $\alpha \sim \omega^3$ of the BW and $\alpha \sim \omega^{3.8}$ of the ESW (R mode wave). This result seems to be quite reasonable because the surface-mode waves are thought to have intermediate characters between the BW and the ESW in the sense that they satisfy a boundary condition at the surface but propagate into the bulk region. For the SH mode wave, the behavior of the gain $\alpha \sim \omega^{3.1}$ at frequencies near 10 GHz is similar to $\alpha \sim \omega^3$ of the BW also for case II. However, at these frequencies the effects of the electronic screening are not considered to be so large for the SH mode, unlike for the other two modes; and the gain is expected to depend on the frequency much steeper at lower frequencies. The frequency dependences of the gains $\alpha \sim \omega^{-1.2}-\omega^{-1.5}$ of the SH mode waves in the high-frequency region near 100 GHz, where the effects of the electronic screening are small, are also stronger than $\alpha \sim \omega^{-1}$ of the bulk shear waves. Furthermore, the frequency dependences $\alpha \sim \omega^{0.5}-\omega^{1.0}$ of the SV-P mode waves near 100 GHz are also interesting in comparison with $\alpha \sim \omega$, which is derived from the deformation-potential coupling for the BW.

We now comment briefly on the applied field or the drift parameter (x) dependences of the amplifications. An analytic expression [Eq. (21)] of the amplification rate has the same x dependence as that of the Rayleigh wave in the Born approximation.[5] Therefore, we may expect that same x dependences of the amplification rate for the surface-mode waves as that of the Rayleigh wave. Numerical calculations have really revealed the behavior of α, which depends on x linearly up to $x \simeq 10$, then begins to deviate from the linear dependence and saturates. However, up to about $x = 30$, which corresponds to the electron drift velocity $v \simeq 10^7$ cm/sec, the deviation from $\alpha \sim x$ is small.

Finally, we remark on an effect of the surface inhomogeneities. The real surface of an expitaxial film is not flat and to some extent has roughness and irregularities. Therefore, even if we project waves to the surface with a fixed incident angle, the reflected waves from the surface do not come out with a uniform reflected angle, but may be distributed around reflection angle θ_R. A gain to be observed experimentally will therefore be an average over a suitable small angle around θ_R of the gains calculated theoretically assuming the ideal surface. The theoretical expressions of the gains have smooth dependence upon the incidence (or reflection) angle. Consequently the values of the amplifications that we have obtained hitherto must not be very different from such averaged values and will be correct even if we consider the effects of the surface roughness and other irregularities apart from the attenuations caused by them and other origins.

ACKNOWLEDGMENTS

One of the authors (S. T.) wishes to express his thanks to the Sakkokai Foundation for financial support. Numerical calculations were performed using the FACOM 230-75 facilities at the Hokkaido University Computing Center.

APPENDIX

For a crystal with high electrical resistivity (i.e., low carrier concentration) we can set the electric displacement $\vec{D}$ equal to a constant (e.g., zero). In this case the electric field $\vec{E}$ is the

fundamental dependent electrical variable, and the piezoelectric equations of state are written in the form

$$E_i = -(4\pi/\epsilon_0)e_{ijk}S_{jk},$$
$$T_{ij} = c^D_{ijkl}S_{kl},$$

where $\{T_{ij}\}$, $\{e_{ijk}\}$, and $\{S_{ij}\}$ are the stress, the piezoelectric, and the strain tensors, respectively, and the summation convention is followed. $\{c^D_{ijkl}\}$ is the elastic stiffness tensor at constant electric displacement and ϵ_0 is the static dielectric constant. At higher carrier concentrations, we must incorporate the electronic screening effects. A component of the electric field is written more explicitly in terms of the displacement vector $\vec{u}$ of a medium:

$$E_i = -\frac{2\pi}{\epsilon_0}e_{ijk}\left(\frac{\partial u_j}{\partial r_k}+\frac{\partial u_k}{\partial r_j}\right). \tag{A1}$$

For a crystal with the zinc-blende crystal structure ($e_{14}=e_{25}=e_{36}=e_P$; other components $e_{ijk}=0$) we can write (A1) explicitly as

$$\begin{aligned}
E_j^{\text{P-SV}} &= -i\frac{4\pi e_P}{\sqrt{2}\,\epsilon_0}(\tau_1)_{jn}k_n\left(\frac{k}{4\pi}\right)^{1/2}\\
&\quad\times[4\delta^{1/2}(e^{-i\delta kz}+De^{i\delta kz})\\
&\quad -2B(\sigma^{3/2}-\sigma^{-1/2})e^{i\sigma kz}]e^{i\vec{k}\cdot\vec{r}},\\
E_z^{\text{P-SV}} &= i\frac{4\pi e_P}{\sqrt{2}\,\epsilon_0}\frac{k_xk_y}{k}\left(\frac{k}{4\pi}\right)^{1/2}\\
&\quad\times[4\delta^{-1/2}(e^{-i\delta kz}-De^{i\delta kz})\\
&\quad +4\sigma^{1/2}Be^{i\sigma kz}]e^{i\vec{k}\cdot\vec{r}},
\end{aligned} \tag{A2}$$

$$\begin{aligned}
E_j^{\text{SV-P}} &= \frac{4\pi e_P}{\sqrt{2}\,\epsilon_0}(\tau_1)_{jn}k_n\left(\frac{k}{4\pi}\right)^{1/2}\\
&\quad\times[4\delta^{1/2}Be^{i\delta kz}\\
&\quad -2(\sigma^{3/2}-\sigma^{-1/2})(e^{-i\sigma kz}-De^{i\sigma kz})]e^{i\vec{k}\cdot\vec{r}},
\end{aligned} \tag{A3}$$

$$\begin{aligned}
E_z^{\text{SV-P}} &= \frac{4\pi e_P}{\sqrt{2}\,\epsilon_0}\frac{k_xk_y}{k}\left(\frac{k}{4\pi}\right)^{1/2}\\
&\quad\times[4\delta^{-1/2}Be^{i\delta kz}\\
&\quad +4\sigma^{1/2}(e^{-i\sigma kz}+De^{i\sigma kz})]e^{i\vec{k}\cdot\vec{r}},
\end{aligned}$$

$$E_j^{\text{SH}} = \frac{4\pi e_P}{\epsilon_0}(\tau_3)_{jn}k_n\left(\frac{2k\sigma c^2}{\pi c_t^2}\right)^{1/2}\sin\sigma kz\; e^{i\vec{k}\cdot\vec{r}}, \tag{A4}$$

$$E_z^{\text{SH}} = -i\frac{4\pi e_P}{\epsilon_0}\frac{k_x^2-k_y^2}{k}\left(\frac{2kc^2}{\pi c_t^2\sigma}\right)^{1/2}\cos\sigma kz\; e^{i\vec{k}\cdot\vec{r}},$$

where $j,n=x,y$ and

$$\tau_1=\begin{pmatrix}0&1\\1&0\end{pmatrix},\quad \tau_3=\begin{pmatrix}1&0\\0&-1\end{pmatrix}.$$

It has been shown[6] that the longitudinal electric field has an effect large enough to be observable in most piezoelectric materials and that the transverse electric field has very little effect on the acoustic waves. If we take the boundary surface as the (001) crystal plane, we see from Eq. (A4) that the SH mode wave with a two-dimensional wave vector $\vec{k}$ pointing in the [110] direction does not produce a longitudinal component of the electric field but, with $\vec{k}$ pointing in the [100] and its equivalent directions, is accompanied with the longitudinal one. This result is due to the fact that the lattice displacement normal to the surface does not exist for the SH mode and is different from that in bulk shear waves. Hereafter, we take the (001) crystal plane as a surface and consider the waves with the propagation vector $\vec{k}$ fixed to the [110] direction for the P-SV and SV-P mode waves and the [010] direction for the SH mode wave.

Noting the configurations of wave propagations depicted in Fig. 2, the longitudinal electric fields of each mode are derivable from the potentials

$$\begin{aligned}
\varphi_J(\vec{r}) &= \frac{8\pi e_P}{\sqrt{2}\,\epsilon_0}\left(\frac{k}{4\pi}\right)^{1/2}\\
&\quad\times\left[3\delta^{1/2}\left(\frac{c_l}{c}\right)^2(e^{-i\delta kz}+De^{i\delta kz})\right.\\
&\quad\left.-B(2\sigma^{3/2}-\sigma^{-1/2})\left(\frac{c_t}{c}\right)^2e^{i\sigma kz}\right]e^{ikx}
\end{aligned} \tag{A5}$$

for the P-SV mode

$$\begin{aligned}
\varphi_J(\vec{r}) &= i\frac{8\pi e_P}{\sqrt{2}\,\epsilon_0}\left(\frac{k}{4\pi}\right)^{1/2}\\
&\quad\times\left[3B\delta^{1/2}\left(\frac{c_l}{c}\right)^2e^{i\delta kz}\right.\\
&\quad\left.-(2\sigma^{3/2}-\sigma^{-1/2})\left(\frac{c_t}{c}\right)^2(e^{-i\sigma kz}-De^{i\sigma kz})\right]e^{ikx}
\end{aligned} \tag{A6}$$

for the SV-P mode, and

$$\varphi_J(\vec{r}) = -i\frac{8\pi e_P}{\epsilon_0}\left(\frac{2k\sigma c^2}{\pi c_t^2}\right)^{1/2}\left(\frac{c_t}{c}\right)^2\sin\sigma kz\; e^{ikx} \tag{A7}$$

for the SH mode, where we have taken the x direction parallel to the wave vector $\vec{k}$. The factor $2\sigma^{3/2}-\sigma^{-1/2}$ in Eqs. (A5) and (A6) vanishes for $\tan\theta_s=\sqrt{2}$, which means that the SV wave traveling in the [111] direction does not produce the longitudinal electric field. This is the same result as in the bulk shear wave and is expected by the plane-wave nature of the P-SV and SV-P waves.

In the phonon picture given in Sec. III the electric potentials are quantized as follows:

$$\tilde{\varphi}(\vec{r})=\sum_J\left(\frac{\hbar}{2\rho\omega_J S}\right)^{1/2} a_J\varphi_J(\vec{r})+\text{H.c.},$$

where summation over J involves the R and the TR modes that we have not considered in this paper. The interaction Hamiltonian of the piezoelectric electron-phonon coupling is written in terms of the potential $\tilde{\varphi}$ and field operators of the electron [Eq. (5)] as

$$H_P=-e\int\psi^\dagger(\vec{r})\tilde{\varphi}(\vec{r})\psi(\vec{r})d\vec{r}.$$

[1]R. E. Prange, Phys. Rev. 187, 804 (1969); H. Ezawa, S. Kawaji, and K. Nakamura, Jpn. J. Appl. Phys. 13, 126 (1974).

[2]T. Nakayama and T. Sakuma, J. Appl. Phys. 46, 2445 (1975); 47, 2263 (1976); A. A. Maradudin and D. L. Mills, Appl. Phys. Lett. 28, 573 (1976); Ann. Phys. (N. Y.) 100, 262 (1976); P. G. Steg and P. G. Klemens, Phys. Rev. Lett. 24, 381 (1970); J. Appl. Phys. 45, 23 (1974); A. J. De Vries and R. L. Miller, Appl. Phys. Lett. 20, 210 (1972); T. Nakayama and T. Sakuma, Lett. Nuovo Cimento 2, 1104 (1971); T. Sakuma, Phys. Rev. Lett. 29, 1394 (1972); Phys. Rev. B 8, 1433 (1973); T. Nakayama, Solid State Commun. 20, 721 (1976); Phys. Rev. B 14, 4670 (1976).

[3]R. Q. Scott and D. L. Mills, Solid State Commun. 18, 849 (1976); S. Maekawa and M. Tachiki, AIP Conf. Proc. 29, 542 (1975).

[4]J. H. Collins and P. J. Hagon, Electronics 42 (10 November), 97 (1969); T. M. Reeder, IEEE Trans. Microwave Theory Tech. 21, 161 (1973).

[5]S. Tamura and T. Sakuma, Solid State Commun. 21, 819 (1977); Phys. Rev. B 15, 4948 (1977).

[6]See, for example, J. W. Tucker and V. W. Rampton, *Microwave Ultrasonics in Solid State Physics* (North-Holland, Amsterdam, 1972), Chap. 7, and references to the original publications cited there.

[7]For GaAs, $E_g=1.51$ eV at $T=77$ K. Throughout this paper, numerical estimates are all performed at $T=77$ K.

[8]H. Ezawa, Ann. Phys. (N. Y.) 67, 438 (1971).

[9]D. K. Dacol and A. H. Zimerman, Phys. Rev. B 11, 974 (1975).

[10]$\tilde{u}_{P\text{-}SV}(\vec{r})$ and $\tilde{u}_{SV\text{-}P}(\vec{r})$ are related to $\tilde{u}_+(\vec{r})$ and $\tilde{u}_-(\vec{r})$ given in Ref. 8 as $\tilde{u}_{P\text{-}SV}=(\tilde{u}_+-\tilde{u}_-)/\sqrt{2}$ and $\tilde{u}_{SV\text{-}P}=(\tilde{u}_++\tilde{u}_-)/\sqrt{2}$.

[11]B. R. Nag, *Theory of Electrical Transport in Semiconductors* (Pergamon, New York, 1972).

[12]Anisotropy ratio $\eta=2c_{44}/(c_{11}-c_{12})=1.80$ for GaAs.

[13]F. I. Fedorov, *Theory of Elastic Waves in Crystals* (Plenum, New York, 1968). The isotropic stiffness constants c_{ij} are approximated from the anisotropic constants c_{ij}' as $c_{11}=c_{11}'-\frac{2}{5}c^*$, $c_{12}=0$, and $c_{44}=c_{44}'+\frac{1}{5}c^*$, where $c^*=c_{11}'-c_{12}'-2c_{44}'$.

[14]M. Neuberger, *Handbook of Electronic Materials* (Plenum, New York, 1971), Vol. 2.